

## Letter to the Editor

# Water ions, dust and CN in comet 46P/Wirtanen<sup>★</sup>

K. Jockers<sup>1</sup>, T. Credner<sup>1</sup>, and T. Bonev<sup>2,★★</sup>

<sup>1</sup> Max-Planck-Institut für Aeronomie, Max-Planck-Str. 2, D-37191 Katlenburg-Lindau, Germany

<sup>2</sup> Institute of Astronomy, Bulgarian Academy of Sciences, Tsarigradsko chausée 72, 1784 Sofia, Bulgaria

Received 23 October 1997 / Accepted 23 January 1998

**Abstract.** Comet 46P/Wirtanen was observed at Pik Terskol (Northern Caucasus) with the 2m-Zeiss-Telescope of the International Centre for Astronomical and Medico-Ecological Investigations, Kiev, on March 10 and 11, 1997. The two-channel focal reducer of the MPAe was used. It allows observations of comets simultaneously in a red and a blue filter passband. The comet was observed with interference filters centered at 615 nm ( $\text{H}_2\text{O}^+$ ) and 388 nm (CN) and with a wide-band red continuum filter. From the March 11 data we have derived an  $\text{H}_2\text{O}^+$  image and an upper limit of the  $\text{H}_2\text{O}^+$  production rate, the CN production rate and the “ $Af\rho$ ” value, indicative of the dust production. The gas to dust ratio is about 2–3 times higher than in comet 1P/Halley.

**Key words:** plasma – gas – dust

### 1. Introduction

Comet 46P/Wirtanen (in the following Wirtanen or P/W) is a member of the Jupiter family of short-period comets. Close encounters with Jupiter (minimum distance in Apr. 1972 was 0.276 AU and in Feb. 1984 0.463 AU, Belyaev et al. 1986) changed its perihelion from 1.63 to 1.06 AU. The comet has been selected as target for the ESA-Rosetta mission. According to present plans the Rosetta spacecraft will make a rendezvous with P/W in 2011 when the comet will be close to aphelion. The spacecraft will then study the comet on its way to perihelion (Oct. 2013).

In order to characterize the comet and set constraints on the spacecraft design P/W was observed on two nights in March 1997, when the comet was close to perihelion. In the first night we observed the comet’s dust coma with a red wide-band filter and with an interference filter transmitting the CN coma at 388 nm. After detection of an ion tail in the exposures with the red filter, in the next night we observed the comet also with an

interference filter transmitting part of the 8–0 band of  $\text{H}_2\text{O}^+$ . This paper presents the results from the second night.

$\text{H}_2\text{O}^+$  column density maps and/or production rates of the following comets have been derived from narrow-band images up to now: 1P/Halley (DiSanti et al. 1990, Scherb et al. 1990) Liller 1988V (Rauer and Jockers 1990, see also Jockers 1991), 10P/Tempel 2 (Rauer and Jockers 1990), Austin 1990 V (Schultz et al. 1993, Bonev and Jockers 1994) and 109P/Swift-Tuttle (Jockers and Bonev 1997). In order to improve our understanding of comet-solar wind interaction and cometary ion photo-chemistry, observations of comets in a wide range of water production rates are desirable. In this respect our observation of  $\text{H}_2\text{O}^+$  in Wirtanen is useful independent of the ESA-Rosetta mission.

### 2. The instrument

The observations were performed with the two-channel focal reducer of the Max-Planck-Institute for Aeronomy attached to the 2m-Ritchey-Chretien-Coudé telescope on Pik Terskol in the Northern Caucasus at an altitude of 3100m. The two-channel focal reducer has been described by Jockers (1997). At the 2m telescope, the red channel provides a field of view of  $7.8 \times 5.2$  arcmin<sup>2</sup> and a scale of 0.81 arcsec pixel<sup>-1</sup>. In the blue channel the field of view is  $7.8 \times 7.8$  arcmin<sup>2</sup> and the scale 1.0 arcsec pixel<sup>-1</sup>. An offset guider driven by stepping motors allows guiding after non-stationary objects like comets. A detailed description of the Pik Terskol observatory and our observing campaign has been given by Jockers and Credner (1997).

### 3. The observations

March 11 was 2.5 days before P/W’s perihelion passage. The heliocentric distance of P/W was 1.06 AU and the geocentric distance 1.52 AU. The phase angle was 40.5°. Table 1 shows the observations used in this study. In the red channel we have two exposures. Both images show cometary dust and water ions. The image taken through the narrow-band filter has some dust contamination. The image taken through the wide-band filter is much more strongly exposed and shows mostly dust coma, but also plasma structures due to the (7–0) and (6–0) bands of

Send offprint requests to: K. Jockers

<sup>★</sup> based on observations obtained at the Terskol Observatory of the Centre for Astronomical, and Medico-Ecological Investigations, Kiev, Ukraine

<sup>★★</sup> Present address: Max-Planck-Institut für Aeronomie

**Table 1.** Mar 11 observations used in this study

Start UT	Duration of exposure [s]	Object	Airmass	Filter
16:42	600	Comet dust	2.60	RX <sup>1</sup>
16:59	1800	Comet CN	3.25	IF390 <sup>2</sup>
17:00	1800	Comet H <sub>2</sub> O <sup>+</sup>	3.29	IF614 <sup>3</sup>
19:08	2	$\omega$ Tau <sup>4</sup>	2.35	IF614 <sup>3</sup>
19:07	5	$\omega$ Tau <sup>4</sup>	2.34	IF390 <sup>2</sup>
19:24	2	26 UMa <sup>4</sup>	1.01	IF614 <sup>3</sup>
19:23	5	26 Uma <sup>4</sup>	1.01	IF390 <sup>2</sup>

<sup>1</sup> Centre wavelength = 6940 Å, FWHM = 790 Å.

<sup>2</sup> Centre wavelength = 3894 Å, FWHM = 105 Å.

<sup>3</sup> Centre wavelength = 6143 Å, FWHM = 32 Å.

<sup>4</sup> Voloshina et al. 1982

H<sub>2</sub>O<sup>+</sup>. The NH<sub>2</sub> bands at 662 and 697 nm are also transmitted by the wide-band filter but, because of their faintness and the short scalelength of NH<sub>2</sub>, are considered unimportant. The most critical step of the data reduction is the removal of continuum from the narrow-band image. As has been pointed out in previous papers (Jockers et al. 1992, Jockers and Bonev 1997) we make use of the fact that in the near-nucleus region the dust has a sharp peak while the plasma is more evenly distributed. In contrast to Jockers and Bonev (1997) we have employed an interference filter free from CO<sup>+</sup> contamination. The data reduction takes into account that the wide-band image also contains H<sub>2</sub>O<sup>+</sup> emission. In order to calculate H<sub>2</sub>O<sup>+</sup> column densities we used half of the *g*-factor provided by Lutz (1987), because only half of the (8–0) band is transmitted by our filter (see Jockers and Bonev 1997).

The CN image was converted to column densities with the *g*-factor provided by Zucconi and Festou (1985). Using the dust image of the red channel, we removed from the CN image the dust continuum. As this is a very minor correction as compared to the strong CN signal, a possible deviation of the dust colour from solar colour can be neglected.

#### 4. H<sub>2</sub>O<sup>+</sup> image and H<sub>2</sub>O<sup>+</sup> flux

The processed H<sub>2</sub>O<sup>+</sup> image (with continuum removed) is shown in Fig. 1. The contours have been smoothed over 2 to 8 pixels, depending on the contour level. The image shows the typical steep gradient at the nucleus in the sunward direction caused by ion pickup. Note that, if the continuum had not been adequately removed, we would notice a centered peak at the nucleus position of positive or negative value.

To obtain an upper limit of the H<sub>2</sub>O<sup>+</sup> production rate we determine the number of ions per tail length. We deproject the image by stretching it in comet-sun direction by  $1/\sin\alpha$  ( $\alpha$  denotes the phase angle) and multiply the column densities with  $\sin\alpha$ . Then we integrate along the columns of the deprojected image. The result is shown in the lower panel of Fig. 2. The rather high values on the solar side of the nucleus are caused by a ghost image of the nucleus (not visible in Fig. 1) and therefore are not

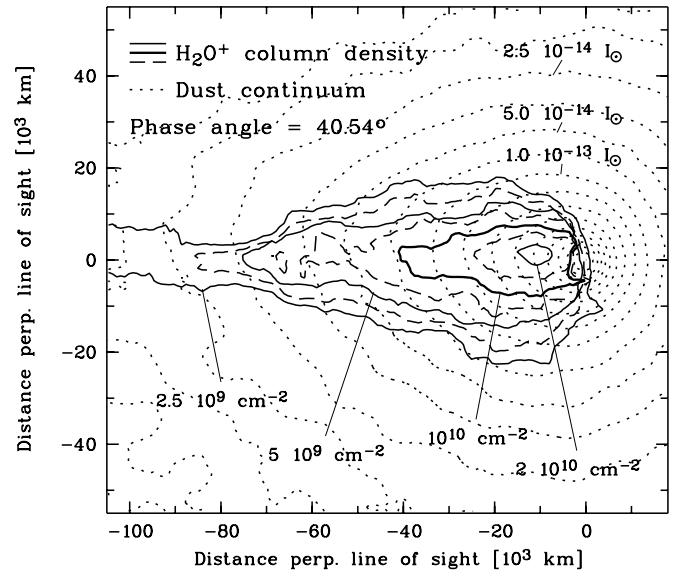


**Fig. 1.** Isocontours of plasma (full and dashed lines) and dust (dotted lines). The contours are labeled in H<sub>2</sub>O<sup>+</sup> ions cm<sup>-2</sup> and mean solar disk intensities  $I_{\odot}$ , respectively. The abscissa is parallel to the comet-sun direction and both coordinates denote distance at the comet perpendicular to line of sight.

real. Outside of the H<sub>2</sub>O<sup>+</sup> source region at distances  $> 10^5$  km tailward of the nucleus the ion flux is conserved (see Jockers and Bonev 1997). If we knew the ion speed averaged over the tail cross-section at a single distance  $> 10^5$  km in the tail we could determine the H<sub>2</sub>O<sup>+</sup> flux and, from flux conservation, the profile of the velocity variation averaged across the tail. No velocity values have ever been measured at distances  $> 10^5$  km in comets with water production rates similar to comet Wirtanen (see Table 2). Because of reduced mass loading caused by the small amount of cometary ions the flow speeds may approach solar wind speed. In any case we can derive an upper limit of the H<sub>2</sub>O<sup>+</sup> production rate if we assume the solar wind speed as an upper limit to the ion speed. At the time of the observations the solar wind was measured by the SoHO spacecraft. SoHO was, however, very far from comet Wirtanen so that a determination of the solar wind speed at Wirtanen from the spacecraft measurements is not possible. CELIAS/PM data (courtesy F. M. Ipavich) show that during the Carrington rotations 1907 and 1908, relevant for our observations, the solar wind speed did not exceed 600 km s<sup>-1</sup>, and we will therefore assume this speed as upper limit for the ion speed in the far tail at the time of our observations. An H<sub>2</sub>O<sup>+</sup> production rate of  $5 \times 10^{26}$  H<sub>2</sub>O<sup>+</sup> ions s<sup>-1</sup> provides as mean value such velocities (see the upper panel of Fig. 2).

#### 5. CN production rate

The CN image was averaged in azimuth with respect to the cometary nucleus. A Haser model (Haser 1957) was fitted to the radial profile. In agreement with Osip et al. (1992, see Schleicher et al. 1987) an outflow speed of 1 km s<sup>-1</sup> was assumed. As the

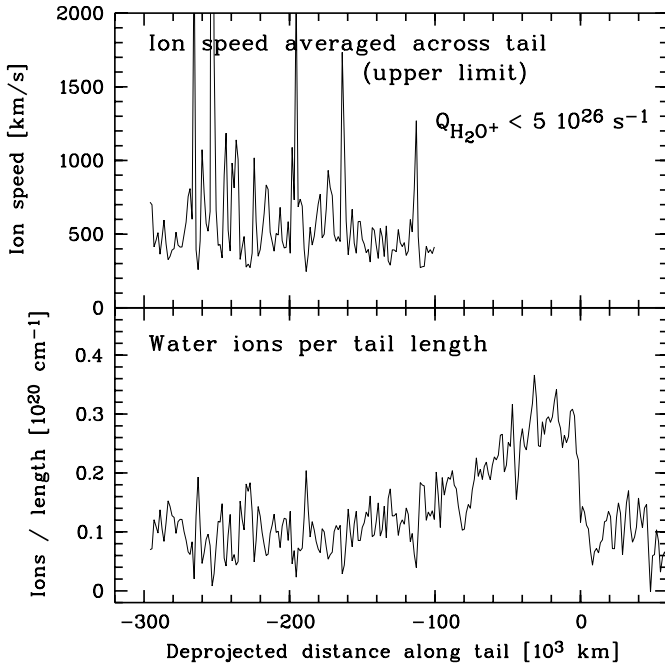


**Fig. 2.** Bottom:  $\text{H}_2\text{O}^+$  content in the tail versus deprojected distance along the tail-Sun direction, derived from observations. Top: Ion speed averaged across tail, derived from bottom panel with a  $\text{H}_2\text{O}^+$  production of  $5 \cdot 10^{26}$  ion  $\text{s}^{-1}$  (see text).

CN coma is very extended and completely fills the frame it is difficult to derive the sky background directly from the CN frame. Therefore, besides of parent scale a correction to the sky background was introduced as free parameter into the Haser fit. Because of the small field of view of  $(3.5 \cdot 10^5 \text{ km})^2$  at the comet the profiles were insensitive to changes of the daughter scalelength, which was taken =  $3 \cdot 10^5 \text{ km}$  (A'Hearn 1982). The best fit is obtained with a parent scale of  $1.83 \cdot 10^4 \text{ km}$  (A'Hearn 1982 gives  $2.2 \cdot 10^4 \text{ km}$ ) and a sky correction equivalent to  $1.3 \cdot 10^9 \text{ CN particles cm}^{-2}$ . A CN production of  $2.85 \cdot 10^{25}$  particles  $\text{s}^{-1}$  was derived.

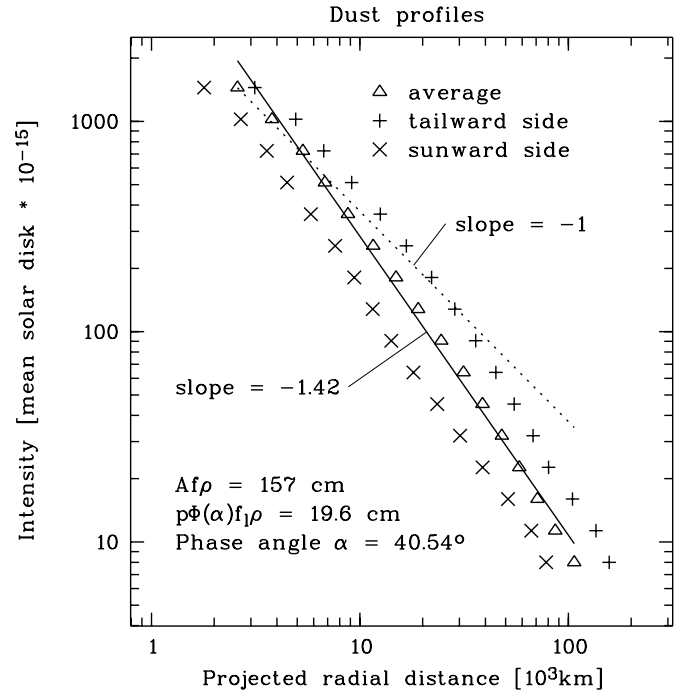
## 6. Dust

Fig. 3 shows a radial profile of the dust image after it was averaged in azimuth like the CN image. A log-log fit to the averaged data gives a rather steep gradient of -1.42, indicative of acceleration by radiation pressure (Jewitt and Meech 1987). To characterize the dust coma of a comet it has become customary to determine the product albedo, filling factor and projected distance ( $Af\rho$ ) from the nucleus. This product is independent of the projected distance if the gradient of the log-log fit equals -1.

The following equation allows to calculate the albedo-filling factor product from the dust image (Jockers et al. 1992, 1993).

$$p\Phi(\alpha)f_l = \frac{i}{i_\odot} \frac{r^2}{R_\odot^2}. \quad (1)$$

$p$  is the geometric albedo,  $\Phi(\alpha)$  the phase function and  $f_l$  the local filling factor at a projected distance  $\rho$  from the nucleus.



**Fig. 3.** Dust intensity with respect to the mean solar disk is plotted versus projected radial distance at the comet. The symbols denote measurements of the sunward, tailward and azimuthally averaged profiles. The full line is the fit to the averaged profile. The dotted line is a fit with slope -1 to the first three data points and is used to calculate the albedo filling factor distance product.

$i/i_\odot$  is the dust intensity measured in units of the mean solar disk (Allen 1973),  $r$  is the heliocentric distance of the comet and  $R_\odot$  the solar radius. If we fit a straight line with slope -1 to the three innermost data points of Fig. 3 we derive  $p\Phi(\alpha)f_l\rho = 19.6 \text{ cm}$ . To compare this number with numbers given by Osip et al. (1992) we must multiply our number with eight (see Jockers and Bonev 1997, footnote 1) and get " $Af\rho$ " = 157 cm.

## 7. Discussion

It is useful to compare our data with results of other authors and with well-studied Comet 1P/Halley. Table 2 shows that our CN production value is in perfect agreement with the observations of Farnham and Schleicher (1997). For the  $\text{H}_2\text{O}/\text{H}_2\text{O}^+$  production rate ratio we get a lower limit of about 20. This is consistent with the value of 33 obtained from the balance of photodissociation and photoionization of  $\text{H}_2\text{O}$ . Comparison with Comet Halley reveals that P/W (as many short-period comets) is about a factor 2–3 less dusty than Halley. We note that this statement refers mostly to the micron-sized dust which scatters efficiently in the visual wavelength range, not to the larger grains which may be dangerous to the ESA-Rosetta mission. Micron-sized dust is removed by gas drag. The larger particles cannot leave the neighbourhood of the nucleus and therefore may have accumulated in periodic comets which have spent already a long time in the inner solar system.

**Table 2.** Observations of 46P/Wirtanen close to perihelion

	Date 1997	Wirtanen	Halley at GIOTTO encounter	Halley Wirtanen
H <sub>2</sub> O <sup>+</sup>	Mar 11	<5 10 <sup>26</sup> a	–	–
H <sub>2</sub> O	Feb 10	7 10 <sup>27</sup> b	5.5 10 <sup>29</sup> c	79
H <sub>2</sub> O	Mar 05	1.2 10 <sup>28</sup> d	5.6 10 <sup>29</sup> e	47
CN	Mar 11	2.9 10 <sup>25</sup> a	1.5 10 <sup>27</sup> e	52
CN	Mar 05	2.7 10 <sup>25</sup> d	1.5 10 <sup>27</sup> e	56
“Afρ”	Mar 11	1.6 10 <sup>2</sup> a	1.9 10 <sup>4</sup> e	119
“Afρ”	Mar 05	1.2 10 <sup>2</sup> d	1.9 10 <sup>4</sup> e	158

<sup>a</sup> this work.

<sup>b</sup> Bertaux 1997.

<sup>c</sup> Krankowski et al. 1986.

<sup>d</sup> Farnham and Schleicher 1997, OH rate × 1.5.

<sup>e</sup> Osip et al. 1992, OH rate × 1.5.

A major problem of production rate determination from cometary narrow-band imaging comes from the fact that an outflow speed must be assumed. For the outflow of CN and OH this speed is determined by the thermal speed of the mother substance. Many authors (including us) take a value of 1 km s<sup>-1</sup>, mostly to allow an easy comparison. For H<sub>2</sub>O<sup>+</sup> we have taken the solar wind speed as upper limit. It is evident that the speed problem must receive more attention in the future. For cometary ions this implies direct measurement of ion velocities via Fabry-Perot interferometry (Rauer and Jockers 1993) and more careful modelling of the solar wind interaction with cometary plasma. For the neutral radicals recent measurements of outflow speeds in the radio range provide useful input.

*Acknowledgements.* We thank N. Karpov, A. Sergeev and A. Andrienko for diligent assistance and help during the observations. The results were processed with the MIDAS software package of the European Southern Observatory.

## References

- A'Hearn M. F., 1982, in: Comets, Wilkening L. L. (ed.), University of Arizona Press, Tucson, AZ, p. 443
- A'Hearn M. F., Schleicher D. G., Feldman P. D., Millis R. L., Thompson D. T., 1984, AJ 89, 579
- Allen C. W., 1973, Astrophysical quantities, Athlone Press, London
- Belyaev N. A., Kresák L., Pittich E. M., Pushkarev A. N., 1986, Catalogue of Short-period orbits, Bratislava
- Bertaux J.-L., 1997, IAU circular 6565
- Bonev T., Jockers K., 1994, Icarus 107, 335
- DiSanti M. A., Fink U., Schultz A. B., 1990, Icarus 86, 152
- Farnham, T. D., Schleicher, D., 1997, IAU circular 6595
- Haser L., 1957, Bull. Acad. Roy. Belg. (Classe Sci.) 43, 740
- Jewitt D. C., Meech K. J., 1987, ApJ 317, 992
- Jockers K., 1991 in A. D. Johnstone ed., Cometary plasma processes, AGU Geophysical monograph, 139
- Jockers, K., 1997, in M. Rodonò, ed., Proceedings JENAM-95 conference, Exp. Astron., in press
- Jockers, K., Bonev, T., Ivanova, V., Rauer, H., 1992 A&A 260,455
- Jockers K., Kiselev N. N., Boehnhardt H., Thomas N., 1993, A&A 268, L9
- Jockers K., Bonev T., 1997, A&A 319, 617
- Jockers K., Credner T., 1997, Sterne und Weltraum 36, 1046
- Krankowski et al., 1986, Nature 321, 326
- Lutz, B. L., 1987, ApJ 315, L147
- Osip D. J., Schleicher, D. G., Millis, R. L., 1992, Icarus 98, 115
- Rauer H., Jockers K., 1990, in C.-I. Lagerkvist et al. (eds), Asteroids, Comets, Meteors III, Uppsala, 417
- Rauer H., Jockers K., 1993, Icarus 102, 117
- Scherb F., Magee-Sauer K., Roesler F. L., Harlander J., 1990, Icarus 86, 172
- Schleicher, D. G., Millis R. L., Birch V. P., 1987, A&A 187, 531
- Schultz D., Scherb F., Roesler F. L., 1993, Icarus 104, 185
- Voloshina, I. B., Glushneva, I. N., Doroshenko, B. T. et al., 1982, Spektrofotometriya yarkih zvezd, Nauka, Moscow, (russ.)
- Zucconi J. M., Festou M. C., 1985, A&A 150, 180